This manuscript was accepted and published by ***Energy & Fuels***, a journal of the American Chemical Society. DOI: 10.1021/ef800868k (http://dx.doi.org/10.1021/ef800868k).

This manuscript was placed into the present public repository with the consent of the Editor of *Energy & Fuels*. Publication data of the final, corrected work:

Várhegyi, G.; Chen, H.; Godoy, S.: Thermal decomposition of wheat, oat, barley and Brassica carinata straws. A kinetic study. Energy Fuels **2009**, 23, 646-652. doi: 10.1021/ef800868k

Thermal Decomposition of Wheat, Oat, Barley and *Brassica Carinata* Straws. A Kinetic Study

Gábor Várhegyi,[†,*] *Honggang Chen,*[‡] *and Sandra Godoy*[§]

[†] Institute of Materials and Environmental Chemistry, Chemical Research Center, Hungarian Academy of Sciences, P.O. Box 17, Budapest 1525, Hungary; [‡] China University of Petroleum, Dongying 257061, China; and [§] School of Engineering and Mathematical Sciences, City University, London EC1V 0HB, UK.

[*] To whom correspondence should be addressed.

E-mail: varhegyi.gabor@ttk.mta.hu, Tel. +36 1 4381148, Fax: +36 1 4381147

ABSTRACT. The slow pyrolysis of four biomass samples was studied by thermogravimetry (TGA) at different heating rates. The samples belonged to different botanical classes/genera and their mineral matter content showed a high variation. A distributed activation energy model (DAEM) was used due to the complexity of the biomass samples of agricultural origin. The common features of their decomposition kinetics were sought by evaluating 12 experiments of four biomasses simultaneously by the method of least squares. Two parallel DAEM reactions with a Gaussian distribution of the activation energies were sufficient for an acceptable fit between the experimental and simulated data. Common means and deviations of the activation energies were required for all the four samples. The reactivity differences between the samples were expressed by the differences between the preexponential factors while the weights of the parallel reactions described further differences between the samples. Altogether 20 unknown model parameters were estimated from 12 experiments. When the method of

least squares was used on the mass loss rate (DTG) curves, one of the obtained partial curves showed a sharp peak with a small variation of E. This was associated with the cellulose decomposition. The other partial curve had a much wider E distribution and was assumed to include the decomposition of hemicellulose, lignin and extractives. The evaluation of the sample mass (TGA) data resulted in wider partial peaks than the ones obtained from the DTG data. To exclude the possibility of any mathematical artifact, the evaluation was also carried out on the analytical integrals of the DTG curves.

Keywords: Biomass; agricultural wastes; thermogravimetry (TGA); distributed activation energy model (DAEM); Ethiopian mustard.

1. Introduction

There is a growing interest in biomass fuels and raw materials due to climatic change problems. There are several ways to increase biomass utilizations, including the use of more agricultural byproducts, and the productions of energy crops. The straws of the main grain crops are the most important in the first category. Hence we studied three straws (wheat, oat, barley) in the present work.

In addition there is an increasing demand for biodiesel due to Directive 2003/30/EC of the European Parliament and to similar measures in other parts of the world. Later, however, concern arose about the energy and CO_2 efficiency of the biodiesel production from oilseed crops.[1] This efficiency can be improved by finding suitable plants and by using the lignocellulosic part of the crop, too, for energy production. *Brassica carinata* (Ethiopian mustard) is a promising crop for Mediterranean climates.[2] Gasol et al.[3] have analyzed the energetic and environmental performance of production and distribution of the Brassica carinata biomass crop as a lignocellulosic fuel and found favorable results. Accordingly a straw sample of a B. carinata crop was included as one of the materials studied.

The thermal decomposition reactions play a crucial role during most biomass utilization processes. (The production of liquid fuels from grains and oilseeds is an exception.) Thermogravimetric analysis (TGA) is a high-precision method for the study of the pyrolysis at low heating rates, under well defined

conditions in the kinetic regime. It can provide information on the partial processes and reaction kinetics.

Obviously the heating rate of a TGA cannot be compared with that of a real combustor. However, the experimental techniques employing high heating rates cannot ensure a well-known sample temperature. At high heating rates the differences between the true and the believed sample temperatures can be extremely high. It would be nice to learn directly dependable information on the pyrolysis kinetics under the conditions of a combustor but we do not have yet precise methods for it. In this situation the slow pyrolysis studies serve as a sort of basic research. On the other hand, there are processes based on the slow heating of biomass (e.g. charcoal making, or processing biomass into torrefied wood) and it is possible to develop further industrial applications based on a slow pyrolysis of biomass materials.

TGA has frequently been employed in the kinetic modeling of the thermal degradation of biomass materials. Due to the complex composition of biomass materials, the conventional linearization techniques of the non-isothermal kinetics are not suitable for the evaluation of the TGA experiments.[4] Therefore the TGA experiments of biomass materials are evaluated nowadays by the non-linear method of least squares (LSQ), assuming more then one reaction.[5-24]

Biomass samples usually contain many different pyrolyzing species. Even the same chemical species may have differing reactivity if their pyrolysis is influenced by other species in their vicinity. Such heterogeneity occurs in other materials, too, e.g. in coals. The assumption of a distribution on the reactivity of the species frequently helps in the kinetic evaluation of the pyrolysis of complex organic samples.[25] The distributed activation energy models (DAEM) have been used for biomass kinetics since 1985.[26-34] Usually a whole experimental curve (TGA, DTG, mass spectrometric intensity of FTIR intensity) is described by a single DAEM reaction. Reynolds, Burnham and Wallman[27,28] used discrete, empirical distribution functions for the activation energy. Since their empirical functions were frequently bimodal, their approach has a similarity to the use of two parallel DAEM reactions.

In two recent works Várhegyi et al.[29] and Becidan et al.[33] employed more than one parallel DAEM reactions for modeling the complexity of the samples. The determination of the unknown model

parameters and the verification of the model were based on the least squares evaluation of series of experiments. This approach led to favorable results and allowed predictions outside the experimental conditions of the experiments used in the parameter determination. Charcoal devolatilization[29] and the thermal decomposition of three biomass wastes[33] were studied in this way. Thus we have only limited knowledge yet on the performance and range of applicability of this type of modeling on biomass materials. One of the aims of the present work was to prove the applicability of this approach on further biomass samples.

Another aim was to explore the common features of the studied samples so that only few model parameters should depend on the particular properties of the given sample. This facilitates the application of the model on other biomass materials. Note that we selected straws with highly different inorganic contents for this work and included a sample (*Brassica carinata*) which is botanically very different from the others.

2. Experimental

2.1. Samples. Wheat, winter barley, oat and B. carinata straws from Spain and Denmark were studied. These biomasses were key samples in an EU project aiming at the reduction of the cost and emission in the combustion of high alkali biofuels. Their combustion properties were extensively examined[35-38] and there is a separate publication about the thermal analysis of their ashes.[39] Table 1 contains the analytical characteristics of the samples.[38,39]

Table 1. Analytical characteristics of the samples[38,39]

Plant	Barley	Brassica carinata	Oat	Wheat
Country of origin	Spain	Spain	Spain	Denmark
Code name	HiAl 5	HiAl 7	HiAl 2	HiAl 10
moisture (% m/m)	13.6	10.6	17.2	15.9
Biomass composition (% m/m, dry basis):				
Ash [a]	7.2	5.1	3.9	6.8
C	45	45	48	46
H	6.0	6.0	6.3	6.1
N	0.8	1.1	0.9	0.6
S	0.19	0.28	0.16	0.15
Al	0.008	0.008	0.006	0.04
Ca	0.39	0.74	0.80	0.34
Fe	0.005	0.007	0.006	0.02
K	2.50	1.70	0.61	1.30
Mg	0.10	0.07	0.08	0.07
Na	0.30	0.01	0.14	0.02
Si	0.82	0.06	0.29	1.50
Cl [b]	1.10	0.06	0.06	0.30
P [b]	0.05	0.17	0.10	0.08
LHV [b]	16.5	16.7	17.4	16.8

[a] at 550°C, after a 20h heating in the presence of oxygen

[b] mineral Cl and P

[c] MJ/kg, dry basis

As the data in Table 1 show, the barley sample had a particularly high K, while that of the oat sample was particularly low. The chlorine and silicon content showed even higher differences. B. carinata

showed a high K content with particularly low amounts of Si and Cl. These differences are expected to highly influence the thermal decomposition of the samples.[40]

The samples were ground and sieved using 0.6 mm sieve and the fraction with particle size under 0.6 mm was used in the experiments.

2.2. Thermogravimetric experiments. A Stanton Redcroft series 760 TGA was employed. Approximately 8 mg samples were distributed evenly in a platinum sample pan of ø 3 mm and heated in nitrogen flow at different heating rates. The choice of the sample size was based on the work of Stenseng et al.[41] who showed that the thermal decomposition of wheat straw has a low enthalpy change and the sample mass can go up to 20 mg in experiments similar to our work. We checked their results by repeating wheat straw experiments with lower sample masses, and did not find sample mass effects, as shown later in the treatment. Besides, the low and high heating rate experiments were described by exactly the same models and model parameters, and in this way nearly the same fit was obtained at low, medium and high heating rates. The domains between 150 and 600°C were used for the kinetic evaluation. The drying section below 150°C and the carbonization and carbonate decomposition above 600°C were not evaluated. The temperature was measured in the sample holder. From 150 to 600°C the measured temperature was a linear function of time with correlation coefficients ≥ 0.9999. The experiments were carried out at three heating rates; the actual heating rates were found to be 10.74±0.01, 22.23±0.01 and 47.37±0.10°C in the domain of investigations. These values were rounded to integers in the text and in the Figures. Note that the kinetic evaluation itself did not use the heating rate values, as outlined in the next paragraph. The sample mass curves were normalized by their values at the beginning of the domain, at 150°C. This corresponds to a dry basis practically.

2.3. Numerical methods. The differential of the sample mass curves (DTG) were determined by the analytical differentiation of smoothing splines, as described by Várhegyi and Till.[42] The RMS difference between the spline function and the measured TGA data was around 2.5 μg. The measured temperature values were also smoothed mildly. The differential equations of the model were solved numerically

along the empirical temperature – time functions, while the numerical integration of the Gaussian distribution function was approximated by a Gauss-Hermite quadrature formula of 180 points.[29,43] The nonlinear least squares minimization was carried out by a variant of the Hook-Jeeves method, which is a slow but simple and dependable direct search algorithm.[44] (The rate of convergence is no longer an issue at this size of numerical problems; none of the calculations of this paper needed more than 30 minutes on an ordinary desktop PC.) The starting values for the non-linear optimization were taken from earlier works.[4,33]

3. Results and discussion

3.1. Common DAEM model for the studied samples. Figure 1 shows the DTG curves of the samples at the highest heating rate of the study. From left to right the peak temperatures in Figure 1 are: 340°C (barley); 349°C (B. carinata); 357°C (wheat) and 367°C (oat). There is a correlation between these values and the potassium content of the samples which can be due to the well known catalytic effects of the inorganic cations on the decomposition.[40] Note that the amount of other catalysts, like iron is negligible in these samples. The thermal behavior may be influenced by other factors, too, among others by the biological differences between these plants. Note that B. carinata is in class Magnoliopsida (dicots) while the other species of this study belong to class Liliopsida (monocots).

The DTG curves of the lignocellulosic materials frequently show a sharp cellulose peak which overlaps more or less with a lower temperature hemicellulose peak. In our work the cellulose and hemicellulose peaks highly overlapped each other due to the high amount of inorganic catalysts.[40] Figure 1 shows that the hemicellulose and cellulose peak of the oat sample is less overlapped than those of the other three straws. One can observe a "shoulder" between the partial peaks of the oat straw around 330°C. This behavior can be due to the lower amount of inorganic materials in this sample. (See Table 1.) The correlation between the existence of this shoulder and the ash content has been known for many years.[40]

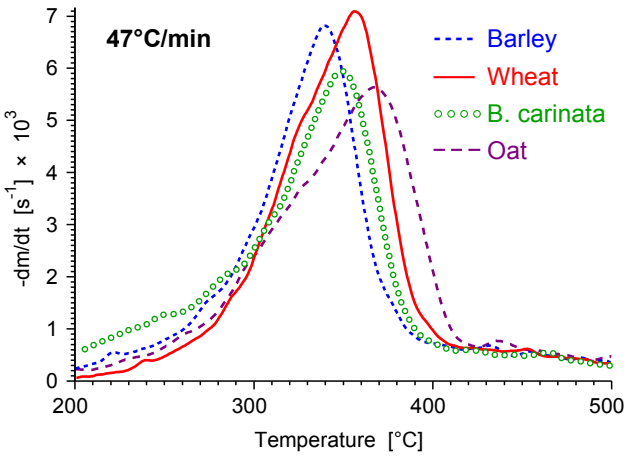

Figure 1. Comparison of the normalized mass loss rates of the samples at the highest heating rate of the study.

Despite the differences in the thermal behavior of these samples, we looked for a common model with a limited number of adjustable parameters. First we evaluated the samples separately from each other by first order, power law and DAEM kinetics in a similar way as in an earlier work.[33] A two-reaction DAEM model was selected from the preliminary calculations for the common evaluation of the four samples. In this model we regarded the straws as the mixture of two pseudo-components. Here a pseudo-component is the totality of those decomposing species which can be described by the same set of reaction kinetic parameters in the given model. Let α_j (j=1, 2) be the reacted fraction of a pseudo-component. The reactivity differences of the reacting species within a given pseudo-component are approximately described by a $Dj(E)$ distribution of the activation energy. Let $\alpha_j(t,E)$ denote the solution of a first order kinetic equation at a given E value:

$$\mathrm{d}\alpha_j(t,E)/\mathrm{d}t = A_j\, \mathrm{e}^{-E/RT}\,[1-\alpha_j(t,E)] \qquad (1)$$

The distribution of E is described by a Gaussian distribution function:

$$D_j(E) = (2\pi)^{-1/2}\,\sigma_{E,j}^{-1}\exp[-(E-E_{0,j})^2/2\sigma_{E,j}^2] \qquad (2)$$

where $E_{0,j}$ and $\sigma_{E,j}$ are the mean value and the width-parameter (variation) of the distribution. The overall reacted fraction of the jth pseudo-component is obtained by integration:

$$\alpha_j(t) = \int_0^\infty D_j(E)\ \alpha_j(t,E)\ \mathrm{d}E \tag{3}$$

The normalized sample mass, m, and its derivative are the linear combinations of $\alpha_j(t)$ and $\mathrm{d}\alpha_j/\mathrm{d}t$, respectively:

$$-\mathrm{d}m/\mathrm{d}t = c_1\,\mathrm{d}\alpha_1/\mathrm{d}t + c_2\,\mathrm{d}\alpha_2/\mathrm{d}t \tag{4}$$

$$m(t) = 1 - c_1\,\alpha_1(t) - c_2\,\alpha_2(\mathrm{d}t) \tag{5}$$

where weight factors c_1 and c_2 are equal to the amount of volatiles formed from pseudo-component 1 and 2, respectively.

In the model we search for common $E_{0,j}$ and $\sigma_{E,j}$ parameters for the four samples while preexponential factors A_j and weight factors c_j were allowed to have different values for the different samples. In this sort of modeling the shape and width of a given partial peak ($\mathrm{d}\alpha_j/\mathrm{d}t$) is similar for all samples at a given heating rate. The position of the partial peaks along the temperature axis and the peak areas have a stronger variation due to the variation of parameters A_j and c_j, respectively.

3.2. Simultaneous evaluation by the method of least squares. As discussed above, we have 20 unknown parameters ($2\,E_{0,j}$, $2\,\sigma_{E,j}$, $8\,A_j$ and $8\,c_j$) to be determined from 12 experiments. The 12 experiments were evaluated simultaneously by the method of least squares by minimizing sum S:

$$S = \sum_{k=1}^{12} \sum_{i=1}^{N_k} \frac{[X_k^{obs}(t_i) - X_k^{calc}(t_i)]^2}{N_k\, h_k^2} \tag{6}$$

Here X^{obs} and X^{calc} denote the observed and simulated values of the quantity evaluated. Subscript k indicates the different experiments. t_i denotes the time values in which the digitized m^{obs} or $(\mathrm{d}m/\mathrm{d}t)^{obs}$ values were taken, and N_k is the number of the t_i points in a given experiment. h_k denotes the heights of the evaluated curves that strongly depend on the experimental conditions. The division by h_k^2 serves for normalization. The fit was characterized by the following quantity:

$$fit\ (\%) = 100\ S^{0.5} \tag{7}$$

Eq 7 is also employed to express the fit of a subgroup within the evaluated experiments. In such cases S is written for the given subgroup. A subgroup may be a single experiment, too.

3.3. Results from the evaluation of the DTG curves. The DTG curves reveal more details on the similarity and differences of the samples than the TG curves. Accordingly we evaluated the DTG curves by substituting X^{obs} and X^{calc} in eq 1 by the corresponding normalized mass loss rate data. This procedure will be called DTG LSQ in the treatment. Good fits were obtained from 150 to ca. 450°C, as shown in Fig. 2. The simulated partial peaks, $d\alpha_1/dt$ and $d\alpha_2/dt$ are also included into Fig. 2. Note that only the results of the highest heating rate of this study, 47°C/min are presented in the figures of the paper. The figures corresponding to heating rates 11 and 22°C/min are shown in the *Supporting Information*. As panel c of Fig 2 indicates, the model did not reproduce the "shoulder" on the oat curve that was discussed in section 3.1. The fit calculated to the three oat experiments by eq 7 was 4.2%, while it was 2.4 – 3.2% for the other samples. In another grouping the fit was found to be 3.3, 3.4 and 3.3% for the 11, 22 and 47°C/min experiments, respectively. The differences between the simulated and the experimental data in the figures indicate that there are no effects of self-cooling or self-heating due to the enthalpy change of the reaction. If there were such effects, the lowest and highest heating rate experiments could not be described by exactly the same parameters. (The reaction rate is roughly proportional with the heating rate. Accordingly the temperature gradients in a given amount of sample are much higher at higher heating rates.) The kinetic parameters are listed in Table 2.

The tall, narrow partial peak, $d\alpha_1/dt$ can be associated with the cellulose pyrolysis according to the data of the literature of biomass pyrolysis.[5-23] Its variance is small ($\sigma_{E,1}$=1.8 kJ/mol), which is in accord with the earlier observations on the first order kinetics of cellulose decomposition. The mean of the activation energy distribution, 167 kJ/mol is lower than the usual activation energy values. This can be due to the catalytic effect of the minerals. In a similar studies on fiberboard, E_0=180 kJ/mol and σ_E=0 kJ/mol was observed for the cellulose peak, which means that the model converged to a simple first order kinetics with a higher activation energy than the corresponding value in the present work.[33]

(Equations 1 - 3 are equivalent to a first order kinetics at $\sigma_{E,j}=0$ since the Gaussian distribution is a Dirac delta function.) However, the mineral matter in that fiberboard sample was only 0.44 % while the samples of the present work contained 3.9 – 7.2% mineral matter. If $d\alpha_1/dt$ is associated with the cellulose decomposition then the second, wider partial peak ($d\alpha_2/dt$) incorporates the pyrolysis of the rest of the sample: hemicellulose, lignin and extractives. Its activation energy range, 226±26 kJ/mol is much higher than the usual activation energies for these components.[12]

We tested how well the model predicts the TGA curves with the parameters obtained from the evaluation of the DTG curves. We got a fit of 1.8% which we displayed in italics in Table 2. (The values corresponding to the least squares minimization are set in boldface there to avoid confusion).

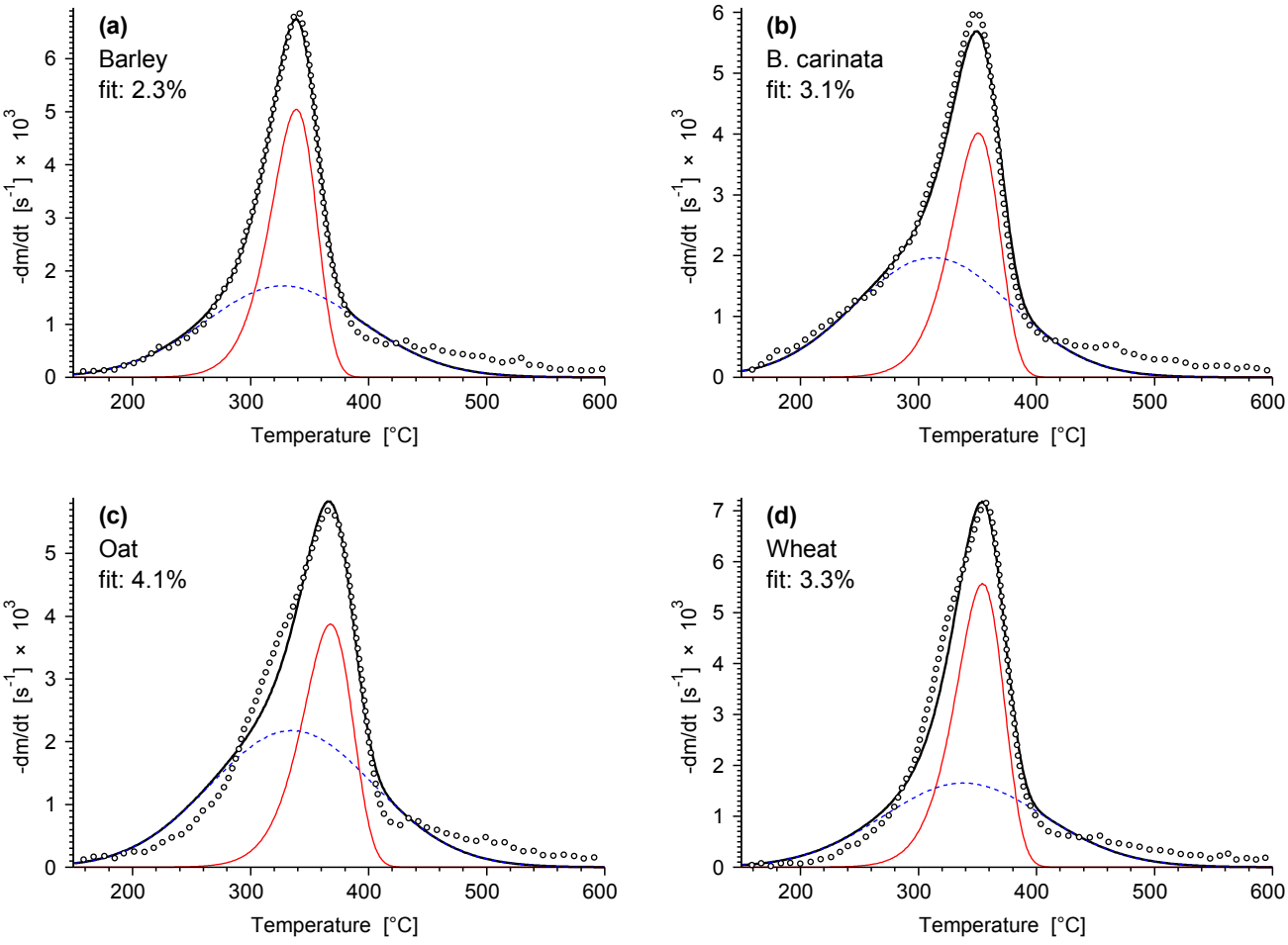

Figure 2. Kinetic evaluation of a series of twelve DTG curves by the method of least squares. The experimental curves (ooo), simulated curves (—) and partial curves (- - -, —) are shown at heating rate 47°C/min. (See Table 2 for the corresponding kinetic parameters.)

Table 2. Kinetic parameters from the Least Squares Evaluation of 12 Experiments

Obtained quantity	Samples [b]	Evaluated quantity [a] DTG	TGA	Spline TGA
fit of DTG data [c] / %	all	**3.32**	*4.88*	*4.89*
fit of TG data [c] / %	all	*1.78*	**0.85**	**0.84**
$E_{0,1}$ / kJ s^{-1}	all	167.3	167.0	167.3
$E_{0,2}$ / kJ s^{-1}	all	225.7	231.5	228.0
$\sigma_{E,1}$ / kJ s^{-1}	all	1.8	4.8	4.8
$\sigma_{E,2}$ / kJ s^{-1}	all	25.9	35.0	34.5
$\log_{10} A_1$ / s^{-1}	barley	12.91	12.97	12.99
$\log_{10} A_2$ / s^{-1}	barley	18.14	17.74	17.44
$\log_{10} A_1$ / s^{-1}	*B. carinata*	12.61	12.74	12.77
$\log_{10} A_2$ / s^{-1}	*B. carinata*	18.71	18.71	18.38
$\log_{10} A_1$ / s^{-1}	oat	12.21	12.40	12.42
$\log_{10} A_2$ / s^{-1}	oat	17.90	17.71	17.40
$\log_{10} A_1$ / s^{-1}	wheat	12.53	12.60	12.62
$\log_{10} A_2$ / s^{-1}	wheat	17.78	17.03	16.73
c_1	barley	0.31	0.41	0.41
c_2	barley	0.36	0.29	0.29
c_1	*B. carinata*	0.26	0.31	0.31
c_2	*B. carinata*	0.41	0.39	0.39
c_1	oat	0.26	0.40	0.40
c_2	oat	0.47	0.35	0.35
c_1	wheat	0.36	0.50	0.50
c_2	wheat	0.35	0.22	0.22

[a] Least squares evaluations were carried out on DTG, TGA and spline-smoothed TGA data. The last one was a special test as outlined in the text.

[b] Part of the parameters were forced to have common values for the four samples while the other ones were allowed to vary from sample to sample.

[c] Boldface indicates the value corresponding to the least squares sum minimized. The values in italics are provided only as additional information.

Table 3. Characteristics of the Simulated Partial Curves at the Highest Heating Rate of this Study, 47°C/min [a]

		Evaluated quantity		
Sample	Characteristics	DTG	TGA	Spline TGA[c]
Barley	$T_{peak,1}$ / °C	339	331	332
	$T_{peak,2}$ / °C	329	349	349
	$FWHM_1$ / °C	46	60	60
	$FWHM_2$ / °C	158	214	214
B. carinata	$T_{peak,1}$ / °C	350	340	340
	$T_{peak,2}$ / °C	313	323	323
	$FWHM_1$ / °C	48	61	61
	$FWHM_2$ / °C	156	205	206
Oat	$T_{peak,1}$ / °C	367	356	356
	$T_{peak,2}$ / °C	334	356	356
	$FWHM_1$ / °C	51	64	64
	$FWHM_2$ / °C	162	217	217
Wheat	$T_{peak,1}$ / °C	354	347	347
	$T_{peak,2}$ / °C	339	371	374
	$FWHM_1$ / °C	48	62	62
	$FWHM_2$ / °C	161	223	224

[a] The peak temperatures (Tpeak) and the peak widths (full width at half maximum, FWHM) of the $d\alpha_1/dt$ and $d\alpha_2/dt$ curves are presented. See Table 2 for the corresponding kinetic parameters.

3.4. Results from the evaluation of the TGA curves. A large number of papers have been published on the kinetic evaluation of the DTG curves of biomass materials. This includes several works that involved the first author of the present paper.[4,5,9,18,20,29,33,40] The difference between the evaluation of

the TGA and the DTG curves is usually not discussed and the systematic errors of the determination of the DTG curves are not analyzed. In the present work we shall deal with these aspects. Accordingly the least squares evaluation of the twelve experiments was also carried out on the TGA curves. In this case X^{obs} and X^{calc} in eq 6 were substituted by normalized sample mass data. This procedure will be called TGA LSQ in the treatment. As Table 2 shows, this approach resulted in a good fit. The quality of the overall fit, as characterized by eq 7, was 0.85%. The $E_{0,1}$ and $E_{0,2}$ values were close to the values obtained from the DTG curves. The relative change of these values was 0.2 and 2.6%, respectively, which is negligible. (Alterations of such magnitudes can easily be compensated by the rest of the parameters. The fit changed from 0.851% to 0.854% only when the $E_{0,1}$ and $E_{0,2}$ values from the DTG LSQ were used as constants in the evaluation of the TGA curves.) However, the width parameters of the activation energy distribution, $\sigma_{E,1}$ and $\sigma_{E,2}$ increased, which led to a substantial increase in the width of the partial peaks. See Table 3 for the peak temperatures and widths of the $d\alpha_1/dt$ and $d\alpha_2/dt$ curves. The change of the widths of the partial curves caused considerable alterations in the c_1 and c_2 values, too.

The calculated results for $\alpha_1(t)$ and $\alpha_1(t)$ partial curves are shown in Figure 3 and in the *Supporting Information*. The corresponding $d\alpha_1/dt$, $d\alpha_2/dt$, $-dm^{calc}/dt$ and $-dm^{obs}/dt$ curves can be found in Figure 4 and in the *Supporting Information*. These figures can directly be compared to the results of the DTG LSQ evaluation. (Cf. Figures 2 and 4). The $-dm^{calc}/dt$ curves of the TGA LSQ evaluation fitted better the flat parts of the $-dm^{obs}/dt$ curves at both ends of the domain of evaluation. On the other hand, the fit was worse at the peak tops. The $-dm^{calc}/dt$ curves of the DTG LSQ evaluation gave a better fit at the higher reaction-rates while they did not describe at all the slow carbonization above ca. 450°C. The overall fit between $-dm^{calc}/dt$ and $-dm^{obs}/dt$ is obviously better at the DTG LSQ evaluation which directly minimizes the deviation between $-dm^{calc}/dt$ and $-dm^{obs}/dt$. (See the corresponding row in Table 2.)

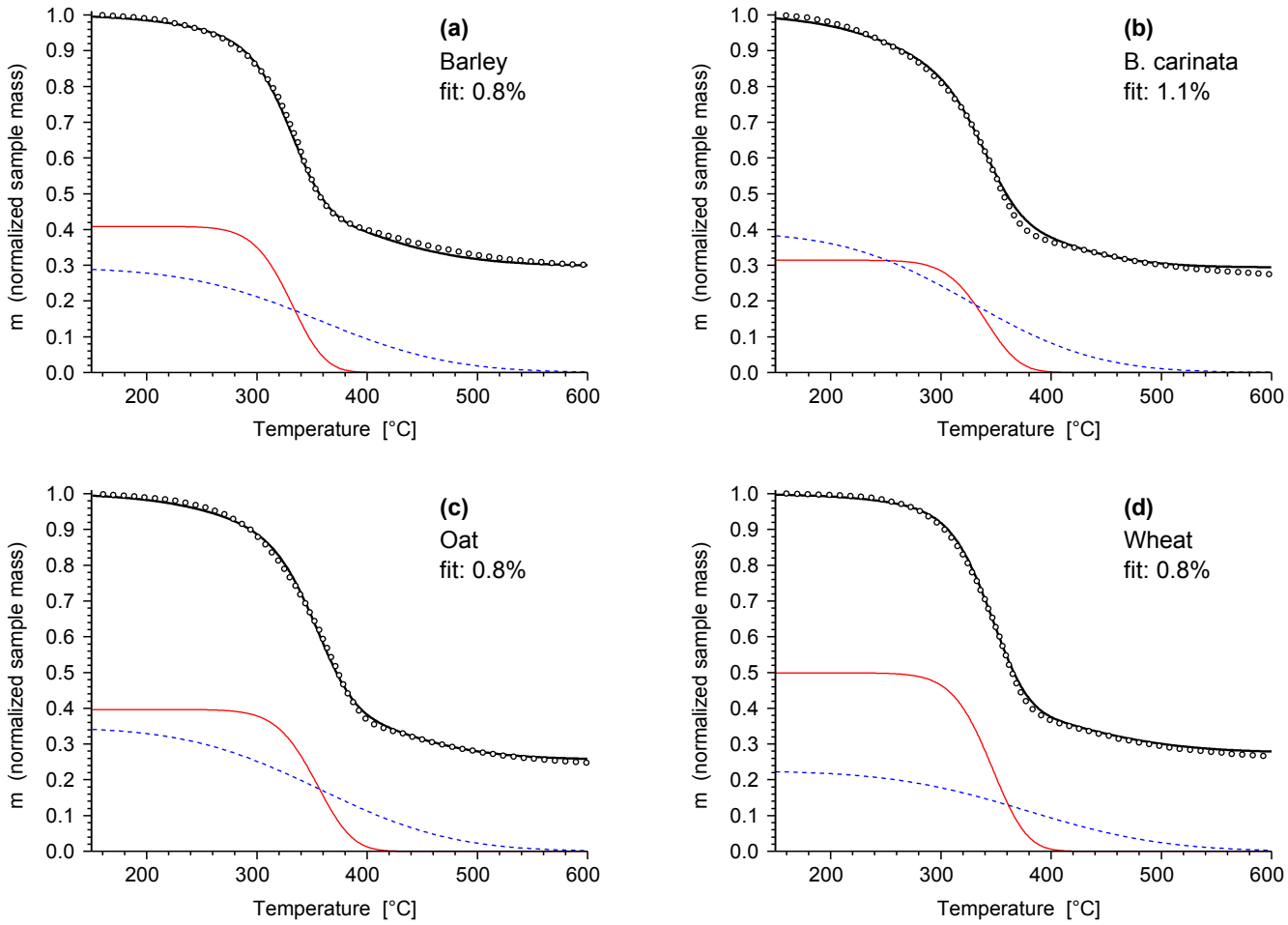

Figure 3. Kinetic evaluation of a series of twelve TGA curves by the method of least squares. The experimental curves (ooo), simulated curves (—) and partial curves (- - -, —) are shown at heating rate 47°C/min. (See Table 2 for the corresponding kinetic parameters.)

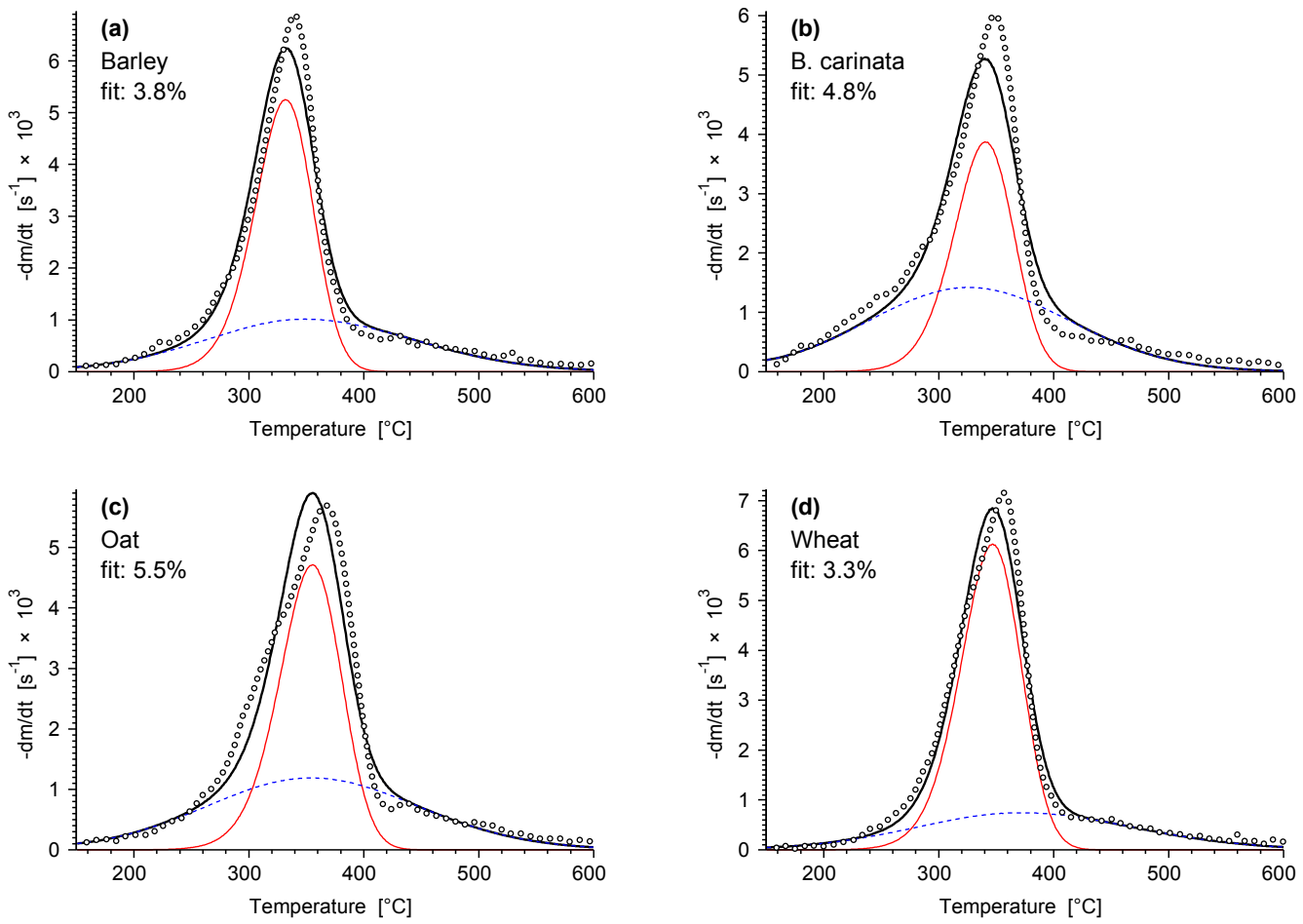

Figure 4. The best fitting parameters of the TGA curves cannot mimic well the top of the experimental DTG peaks. The parameters belonging to Fig. 3 were tested on the corresponding DTG curves. (See Fig 3 for notations.)

3.5. On the difference between the DTG LSQ and TGA LSQ evaluations. From a mathematical point of view the TGA and the DTG curves are not equivalent: the determination of the latter one involves a smoothing procedure. As mentioned in the Experimental, we used smoothing splines for this purpose. The analytical differentiation of these splines provides the $-\mathrm{d}m^{\mathrm{obs}}/\mathrm{d}t$ curves and, obviously, the analytical integration of $-\mathrm{d}m^{\mathrm{obs}}/\mathrm{d}t$ with condition m(0)=1 gives back the smoothing splines. In a test calculation we employed the method of least squares on the smoothing splines instead of $m^{\mathrm{obs}}(t)$. As the data of Tables 2 and 3 show, this approach gave almost the same results as the TGA LSQ evaluation. If the smoothing procedure had caused a significant distortion then the evaluation of the smoothing splines

would have provided results significantly different from those of the TGA LSQ evaluation. Accordingly the difference between the results of the DTG LSQ and TGA LSQ calculations can be due to the different definition of the object function in the least squares optimization. We cannot tell which approach is the better; the usefulness of a model depends obviously both on its accuracy and on the interests of the investigator. If the description of the slow carbonization at the higher temperatures is important then TGA LSQ is more suitable. Otherwise the DTG LSQ approach may be more advantageous. We would like to emphasize that the least squares evaluation does not have maximum likelihood properties in the thermal analysis since the most important experimental errors are not statistical.[4,18] Its best use is as a practical method to ensure the good fit between the experimental and the simulated data.

4. Conclusions

Straw samples were studied by TGA in inert gas flow at different heating rates. The samples revealed different thermal behaviors due to the botanical class/genus differences and also to the sizeable differences in their mineral content. In spite of these differences, the thermal decomposition of the samples could be described by a common model with several common parameters.

Twelve experiments on four samples were evaluated simultaneously by the method of least squares. It is well known that the agricultural by-products contain a wide variety of decomposing species and the catalytic activity of the inorganic ions increases further this diversity. We used a distributed activation energy model to describe this diversity. The model contained two parallel DAEM reactions with Gaussian distribution of the activation energy. The means and width parameters of the activation energy were common parameters for the four samples while the preexponential factors and the weights of the partial reactions were allowed to vary from sample to sample. In this way have two partial curves that are the same for all the four samples. For each partial curve we have a parameter that practically determines the peak position along the temperature axis and a scale factor that determines the peak height. This feature facilitates the application of the model for other samples since only four parameters

depend on the properties of the given straw. Another aspect of the work is the well-conditioned kinetic evaluation. 20 unknown parameters were determined from 12 experiments, meaning an average of only 1.7 unknown per experiment. Good agreement was obtained between the experimental data and the data simulated from the model in this way.

The least squares evaluation was carried out on the DTG and TGA data in separate calculations. The means of the activation energy distributions were nearly the same in the two cases but the rest of the parameters showed ample differences. To exclude the possibility of any mathematical artifact, the evaluation was also carried out on the analytical integrals of the DTG curves. Since the method of least squares does not have a statistical background in the evaluation of thermal analysis experiments, the choice between the evaluation of the DTG and TGA curves can be based on practical considerations. If the good description of the high reaction rate regions of the process is important for the investigator then the evaluation of the DTG curves is advisable.

Acknowledgment. This work was founded by European Union Research Project: HIAL – Biofuels for CHP plants – Reduced Emissions and Cost Reduction in the Combustion of High Alkali Biofuels (ENK5-CT2001-000517)., the Chinese – Hungarian Intergovernmental Science & Technology Cooperation Program (CHN-35/2005) and the Hungarian National Research Fund (OTKA K72710).

Supporting Information Available: Figures illustrating the results at heating rates 11 and 22°C/min. This material is available free of charge via the Internet at http://pubs.acs.org.

NOMENCLATURE

α_j reacted fraction of a pseudocomponent

A_j pre-exponential factor (s^{-1})

c_j normalized mass of volatiles formed from a pseudocomponent

$E_{0,j}$ mean activation energy in a distributed activation energy model (kJ/mol)

fit 100 $S^{0.5}$ (%)

h_k height of an experimental curve

m normalized sample mass (dimensionless)

$m^{calc}(t)$ normalized sample mass calculated from a model

$m^{obs}(t)$ mass of the sample divided by the initial sample mass

N_k number of evaluated data on the kth experimental curve

R gas constant (8.3143×10^{-3} kJ mol^{-1} K^{-1})

$\sigma_{E,j}$ width parameter (variance) of Gaussian distribution

S least squares sum

t time (s)

T temperature (°C, K)

Subscripts:

i digitized point on an experimental curve

j pseudocomponent

k experiment

REFERENCES

(1) Pimentel, D.; Patzek, T. W. Ethanol production using corn, switchgrass, and wood; biodiesel production using soybean and sunflower. *Nat. Resour. Res.* **2005**, 14, 65 – 76.

(2) Cardone, M.; Mazzoncini, M.; Menini S.; Senatore, A.: Brassica carinata as an alternative oil crop for the production of biodiesel in Italy: agronomic evaluation, fuel production by transesterication and characterization. *Biomass Bioenergy* **2003**, *25*, 623-636.

(3) Gasol, C. M.; Gabarrell, X.; Anton, A.; Rigola, M.; Carrasco, J.; Ciria, P.; Solano, M. L.; Rieradevall, J. Life cycle assessment of a Brassica carinata bioenergy cropping system in southern Europe. *Biomass and Bioenergy* **2007**, *31*, 543-555.

(4) Várhegyi, G. Aims and methods in non-isothermal reaction kinetics. *J. Anal. Appl. Pyrolysis* **2007**, *79*, 278-288.

(5) Várhegyi, G; Antal Jr, M.J.; Székely, T.; Szabó, P. Kinetics of the thermal decomposition of cellulose, hemicellulose, and sugarcane bagasse. *Energy Fuels* **1989**, *3*, 329-335.

(6) Cozzani, V.; Petarca, L.; Tognotti, L. Devolatilization and pyrolysis of refuse derived fuels: characterization and kinetic modelling by a thermogravimetric and calorimetric approach. *Fuel* **1995**, *74*, 903-912.

(7) Caballero, J. A.; Conesa, J. A.; Font, R.; Marcilla, A. Pyrolysis Kinetics of Almond Shells and Olive Stones Considering their Organic Fractions. *J. Anal. Appl. Pyrol.* **1997,** *42*, 159-175.

(8) Teng, H.; Lin, H. C., Ho, J. A. Thermogravimetric Analysis on Global Mass Loss Kinetics of Rice Hull Pyrolysis. *Ind. Eng. Chem. Res.* **1997**, *36*, 3974-3977.

(9) Várhegyi, G; Antal Jr, M.J.; Jakab, E.; Szabó, P. Kinetic modeling of biomass pyrolysis. *J. Anal. Appl. Pyrolysis* **1997**, *42*, 73-87.

(10) Órfão, J. J. M.; Antunes, F. J. A.; Figueiredo, J. L. Pyrolysis Kinetics of Lignocellulosic Materials - 3 Independent Reactions Model. *Fuel* **1999**, *78*, 349-358.

(11) Helsen, L.; Van den Bulck, E. Kinetics of the low-temperature pyrolysis of chromated copper arsenate-treated wood. *J. Anal. Appl. Pyrolysis* **2000**, *53*, 51-79.

(12) Garcìa-Pèrez, M.; Chaala, A.; Yang, J.; Roy, C. Co-pyrolysis of sugarcane bagasse with petroleum residue. Part I: thermogravimetric analysis. *Fuel* **2001**, *80*, 1245-1258.

(13) Sørum, L.; Grønli, M.G.; Hustad, J.E. Pyrolysis characteristics and kinetics of municipal solid wastes. *Fuel* **2001**, *80*, 1217-1227.

(14) Vamvuka, D.; Pasadakis, N.; Kastanaki E. Kinetic Modeling of Coal/Agricultural By-Product Blends. *Energy Fuels* **2003**, *17*, 549 -558.

(15) Müller-Hagedorn, M; Bockhorn, H.; Krebs, L.; Müller. U. A comparative kinetic study on the pyrolysis of three different wood species. *J. Anal. Appl. Pyrolysis* **2003**, *68-69*, 231-249.

(16) Manyà, J. J.; Velo, E.; Puigjaner, L. Kinetics of biomass pyrolysis: A reformulated three-parallel-reactions model. *Ind. Eng. Chem. Res.* **2003**, *42*, 434-441.

(17) Jauhiainen, J.; Conesa, J.A.; Font, R.; Martin-Gullon, I. Kinetics of the pyrolysis and combustion of olive oil solid waste. *J. Anal. Appl. Pyrolysis* **2004**, *72*, 9-15.

(18) Mészáros, E.; Várhegyi, G.; Jakab, E.; Marosvölgyi, B. Thermogravimetric and reaction kinetic analysis of biomass samples from an energy plantation. *Energy Fuels* **2004**, *18*, 497-507.

(19) Branca, C.; Albano A.; Di Blasi, C. Critical evaluation of global mechanisms of wood devolatilization. *Thermochim. Acta* **2005**, *429*, 133-141.

(20) Gómez, C. J.; Várhegyi, G.; Puigjaner, L. Slow pyrolysis of woody residues and an herbaceous biomass crop: A kinetic study. *Ind. Eng. Chem. Res.* **2005**, *44*, 6650-6660.

(21) Skodras, G.; Grammelis, O. P.; Basinas, P.; Kakaras, E.; Sakellaropoulos, G. Pyrolysis and combustion characteristics of biomass and waste-derived feedstock. *Ind. Eng. Chem. Res.* **2006**, *45*, 3791-3799.

(22) Yang, H; Yan, R.; Chen, H.; Zheng, C.; Lee D.H.; Liang, D.T. In-depth investigation of biomass pyrolysis based on three major components: hemicellulose, cellulose and lignin. *Energy Fuels* **2006**, *20*, 388-393.

(23) Müller-Hagedorn, M.; Bockhorn, H. Pyrolytic Behaviour of different biomasses (angiosperms) (maize plants, straws, and wood) in low temperature pyrolysis. *J. Anal. Appl. Pyrolysis* **2007**, *79*, 136-146.

(24) Cai, J.; Liu, R. Application of Weibull 2-mixture model to describe biomass pyrolysis kinetics. Energy Fuels, **2008**, *22*, 675–678.

(25) Burnham, A. K.; Braun, R. L. Global kinetic analysis of complex materials. *Energy Fuels* **1999**, *13*, 1-22.

(26) Avni, E.; Coughlin, R.W.; Solomon P.R., King H.H.: Mathematical modelling of lignin pyrolysis. *Fuel* **1985**, *64* 1495-1501.

(27) Reynolds, J. G.; Burnham, A. K. Pyrolysis decomposition kinetics of cellulose-based materials by constant heating rate micropyrolysis. *Energy Fuels* **1997**, *11*, 88-97.

(28) Reynolds, J. G.; Burnham, A. K.; Wallman, P. H. Reactivity of paper residues produced by a hydrothermal pretreatment process for municipal solid wastes. *Energy Fuels* **1997**, *11*, 98-106.

(29) Várhegyi, G.; Szabó, P.; Antal, M. J., Jr. Kinetics of charcoal devolatilization. *Energy Fuels* **2002**, *16*, 724-731.

(30) de Jong, W.; Pirone, A.; Wójtowicz, M. A. Pyrolysis of Miscanthus Giganteus and wood pellets: TG-FTIR analysis and reaction kinetics. *Fuel* **2003**, *82*, 1139–47.

(31) Wójtowicz, M. A.; Bassilakis, R.; Smith, W. W.; Chen, Y.; Carangelo, R. M. Modeling the evolution of volatile species during tobacco pyrolysis. *J. Anal. Appl. Pyrolysis*, **2003**, *66*, 235-261.

(32) Rostami, A. A.; Hajaligol, M.R.; Wrenn, S. E. A biomass pyrolysis sub-model for CFD applications. *Fuel* **2004**, *83*, 1519–25.

(33) Becidan, M.; Várhegyi, G.; Hustad, J. E.; Skreiberg, Ø. Thermal decomposition of biomass wastes. A kinetic study. *Ind. Eng. Chem. Res.* **2007**, *46*, 2428 - 2437.

(34) Cai, J. M.; Liu, R. H. New distributed activation energy model: Numerical solution and application to pyrolysis kinetics of some types of biomass. *Bioresource Technol.* **2008,** *99*, 2795–2799.

(35) Wolf, K. J.; Smeda, A.; Müller, M.; Hilpert, K. Investigations on the influence of additives for SO_2 reduction during high alkaline biomass combustion. *Energy Fuels* **2005,** *19,* 820-824

(36) Glazer, M. P.; Khan, N. A.; de Jong, W.; Spliethoff, H.; Schürmann, H.; Monkhouse, P. Alkali metals in circulating fluidized bed combustion of biomass and coal: measurements and chemical equilibrium analysis. *Energy Fuels* **2005**, *19*, 1889 -1897.

(37) Glazer, M. P. Alkali metals in combustion of biomass with coal. PhD Thesis, Technical University Delft, 2006. Available at http://repository.tudelft.nl/file/467832/371841 .

(38) Müller, M.; Wolf, K. J.; Smeda, A.; Hilpert, K. Release of K, Cl, and S species during co-combustion of coal and straw. *Energy Fuels* **2006,** *20,* 1444 -1449.

(39) Arvelakis, S.; Jensen, P. A.; Dam-Johansen, K. Simultaneous thermal analysis (STA) on ash from high-alkali biomass. *Energy Fuels,* **2004**, *18*, 1066 -1076

(40) Várhegyi, G.; Jakab, E.; Till, F.; Székely, T. Thermogravimetric - mass spectrometric characterization of the thermal decomposition of sunflower stem. *Energy Fuels* **1989**, *3*, 755-760.

(41) Stenseng, M; Jensen, A.; Dam-Johansen, K. Investigation of biomass pyrolysis by thermogravimetric analysis and differential scanning calorimetry. *J. Anal. Appl. Pyrolysis* **2001**, *58-59*, 765-780.

(42) Várhegyi, G.; Till, F. Computer processing of thermogravimetric - mass spectrometric and high pressure thermogravimetric data. Part 1. Smoothing and differentiation. *Thermochim. Acta* **1999**, *329*, 141-145.

(43) Donskoi, E.; McElwain, D. L. S. Optimization of coal pyrolysis modeling. *Combust. Flame* **2000**, *122*, 359-367.

(44) Kolda, T. G.; Lewis, R. M.; Torczon, V. Optimization by direct search: New perspectives on some classical and modern methods. *SIAM Rev.* **2003**, 45, 385-482.